ICON Journal of Engineering Applications of Artificial Intelligence
Volume 02 | Issue 04 | 2026
e-ISSN: 3051-3820
p-ISSN: 3051-3812
Journal homepage: https://iconpublishers.com/icon-j-eng-app-ai/

Research Article **DOI: 10.5281/zenodo.19827940**

Design of a Distributed Early Warning and Cueing Network for Long-Range Loitering Munition Target Acquisition Using Ground Sensor Grids

***Abubakar Surajo Imam [1], Aliyu Surajo [2], Bishir Sirajo [3], Muhammad Ahmad Baballe [4]**
[1,2,4] Department of Mechatronics Engineering, Nigerian Defence Academy, Kaduna, Nigeria.
[3] School of General Studies, Federal University of Transportation, Daura, Katsina State, Nigeria.

Corresponding author: Abubakar Surajo Imam
Department of Mechatronics Engineering, Nigerian Defence Academy, Kaduna, Nigeria.

Received Date: 21 March 2026
Published Date: 27 April 2026

Abstract
This paper presents the design and validation of a distributed early-warning and cueing network for long-range loitering munition target acquisition using RA-IDS-type ground sensor grids, probabilistic edge-fusion gateways, and endurance-class airborne ISR confirmation platforms. The proposed architecture transforms terrain-level anomaly detections into structured sensor-to-decision intelligence through a hierarchical trigger–fusion–cueing pipeline that supports persistent corridor surveillance in infrastructure-limited and GNSS-degraded operational environments. A multi-modal sensing model integrating passive infrared, radio-frequency, acoustic, magnetic, and electro-optical channels enable robust anomaly detection across heterogeneous terrain conditions, while neighbourhood consensus validation reduces false-alarm propagation prior to airborne tasking. A probabilistic cue-ranking framework is introduced to prioritise candidate targets using detection confidence, spatial persistence, and corridor relevance metrics, enabling adaptive ISR resource allocation across distributed monitoring sectors. Analytical coverage modelling establishes deployment-density conditions required for persistent corridor observability, and a sensor-to-platform latency model demonstrates substantial reductions in response time relative to conventional airborne-only search workflows. Simulation results show improvements of 72% in decision latency, 31% in detection persistence, 26% in cue stability, and 63% in communication bandwidth efficiency. Experimental validation using the HATSABIBI-26A endurance-class UAV platform confirms reliable cue-directed waypoint retasking performance and stable monitoring continuity under distributed trigger-grid guidance. The proposed framework provides a scalable foundation for next-generation distributed ISR architectures supporting corridor monitoring, infrastructure protection, and civilian-protection-aligned early-warning deployments without requiring persistent overhead surveillance coverage.

Keywords: Distributed early-warning systems; ground sensor grids; loitering munition target acquisition; distributed ISR; sensor fusion; probabilistic cue prioritisation; corridor surveillance; GNSS-denied navigation; endurance UAVs; ISR–strike integration.

I. INTRODUCTION

Modern ISR architectures increasingly rely on layered sensing frameworks integrating ground-based detection infrastructure with endurance-class aerial verification platforms to maintain persistent situational awareness across extended surveillance corridors [7]–[11]. Traditional airborne-centric monitoring approaches suffer from revisit-interval limitations and terrain-masking discontinuities that reduce anomaly detection reliability in infrastructure-limited operational theatres [12]–[15]. Distributed Unattended Ground Sensor (UGS) networks address these limitations by providing continuous terrain-layer detection capability independent of airborne platform availability [16]–[19]. When integrated with endurance-class loitering surveillance platforms, these networks enable cue-directed monitoring workflows that significantly reduce search-driven ISR burden [20]–[23]. Recent advances in probabilistic navigation architectures

further support corridor-scale monitoring under GNSS-degraded conditions by enabling cooperative localisation across heterogeneous sensing layers [2]. Passive multi-modal sensing frameworks combining acoustic, magnetic, RF and infrared signatures improve anomaly detection robustness in contested surveillance environments [3].

Swarm-enabled ISR coordination strategies extend monitoring scalability by supporting distributed task allocation across sensing layers and airborne verification assets [4]. Embedded artificial intelligence perception modules deployed onboard lightweight surveillance UAV platforms further enhance classification reliability following cue-triggered retasking operations [5]. Secure command-and-control data links remain essential for maintaining sensor-to-platform communication continuity in contested electromagnetic environments [1]. Energy-aware trajectory optimisation strategies further reinforce cue-directed deployment efficiency by reducing unnecessary patrol-pattern flight time across extended monitoring corridors [6]. This paper proposes a distributed early warning and cueing network architecture integrating RA-IDS-type ground sensor grids with endurance-class loitering munition platforms through probabilistic sensor fusion and hierarchical ISR–strike communication pipelines.

II. System Architecture Overview

The proposed distributed early-warning and cueing network adopts a layered sensor–fusion and ISR tasking architecture designed to support persistent corridor surveillance and responsive target acquisition for endurance-class loitering munition operations. Such layered sensing frameworks are increasingly recognised as essential components of distributed intelligence, surveillance, and reconnaissance (ISR) systems operating across infrastructure-limited environments where airborne platforms alone cannot guarantee continuous coverage [7]–[11]. The architecture integrates terrain-level anomaly detection, edge-level probabilistic cue validation, and airborne confirmation layers within a unified sensor-to-decision pipeline suitable for GNSS-degraded and communications-constrained operational theatres [2], [3], [12]. As illustrated in Fig. 1, the system is organised into three functional layers forming a hierarchical detection-to-decision pipeline linking distributed ground trigger grids with airborne ISR confirmation platforms through probabilistic fusion gateways [17]–[23].

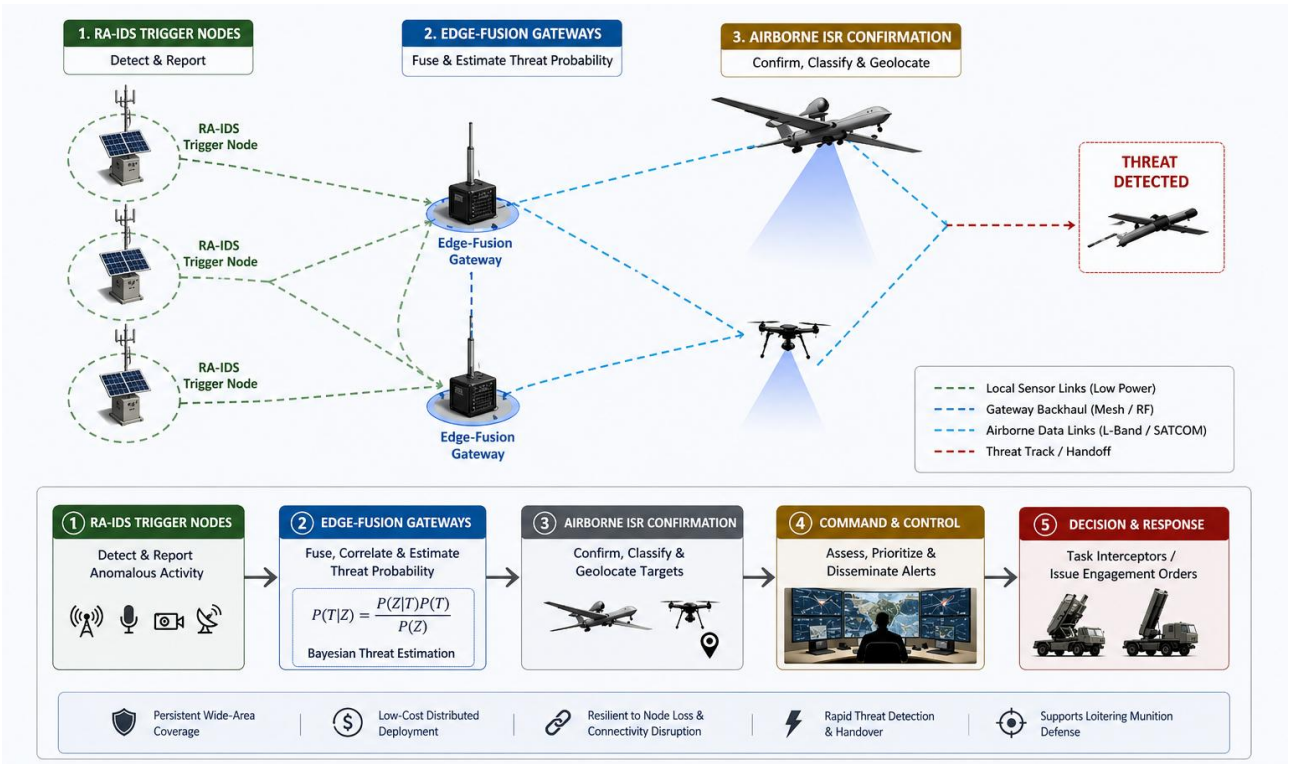

Fig. 1. *Distributed corridor surveillance architecture integrating RA-IDS trigger nodes, probabilistic edge-fusion gateways, and airborne ISR confirmation platforms within a hierarchical sensor-to-decision early-warning framework supporting long-range loitering munition target acquisition.*

A. Ground Trigger Detection Grid

The lowest layer consists of spatially distributed RA-IDS-type multi-modal sensing nodes deployed along surveillance corridors to provide continuous terrain-level monitoring. Distributed unattended ground sensor (UGS) networks significantly improve detection persistence and reduce revisit-interval limitations associated with airborne-only ISR architectures [13]–[16]. These nodes operate as autonomous trigger generators capable of detecting anomalous movement signatures without reliance on persistent airborne coverage. Their distributed deployment ensures detection continuity under terrain masking, intermittent communications, and GNSS-degraded navigation conditions [3], [17].

Each sensing node is represented as a multi-modal detection vector:

$$S_i = \{z_{PIR}, z_{RF}, z_{AC}, z_{MAG}, z_{EO}\}$$

where z_{PIR}, z_{RF}, z_{AC}, z_{MAG}, and z_{EO}denote passive infrared, radio-frequency, acoustic, magnetic, and electro-optical sensing channels, respectively. Multi-modal sensing architectures improve anomaly-detection robustness by combining complementary environmental signatures and reducing susceptibility to single-sensor false-alarm propagation in cluttered surveillance environments [18]–[21].

B. Edge-Level Probabilistic Fusion Gateways

The intermediate layer consists of edge-processing gateways responsible for neighbourhood-level trigger validation and confidence-weighted cue generation. As shown in **Fig. 1**, these gateways form the transition interface between raw sensing activity and actionable ISR tasking information by aggregating detection outputs from adjacent sensor nodes and applying probabilistic fusion logic to suppress spurious triggers prior to transmission to higher decision layers. Distributed probabilistic fusion at the network edge enables early filtering of false detections and reduces communication overhead across large monitoring sectors [22]–[25]. Edge-level processing architectures have been widely adopted in modern distributed sensor networks to enhance scalability, reduce latency, and improve resilience in contested electromagnetic environments [26]–[29]. This distributed processing strategy also supports robust operation when centralised fusion infrastructure is unavailable or degraded [1].

C. Airborne ISR Confirmation Platforms

The upper layer comprises endurance-class unmanned aerial surveillance platforms tasked dynamically using validated cues generated by the fusion layer. As illustrated in Fig. 1, cue-directed deployment enables airborne platforms to operate as responsive verification assets rather than persistent search platforms, thereby improving monitoring efficiency across geographically dispersed surveillance corridors [30]–[33]. Such architectures transform surveillance operations from platform-centric search paradigms into trigger-driven response frameworks aligned with modern distributed ISR concepts and multi-domain sensing integration strategies [34]–[37]. Probabilistic navigation architectures further enable reliable airborne cue exploitation under GNSS-degraded conditions typical of contested operational environments [2], while embedded onboard perception frameworks improve classification confidence following cue-triggered retasking [5]. Energy-aware trajectory optimisation strategies additionally support efficient endurance-class ISR deployment across extended monitoring corridors [6].

III. Multi-Modal Trigger Fusion Model

Reliable anomaly detection in distributed corridor-monitoring environments requires the integration of heterogeneous sensing modalities in order to mitigate single-sensor uncertainty and suppress false-alarm propagation. The proposed architecture therefore employs a multi-modal probabilistic trigger-fusion framework in which complementary sensing channels jointly contribute to a composite detection confidence estimate at each distributed sensor node. Let the sensing vector associated with node S_i be defined as:

$$S_i = \{z_{PIR}, z_{RF}, z_{AC}, z_{MAG}, z_{EO}\},$$

where z_{PIR}, z_{RF}, z_{AC}, z_{MAG}, and z_{EO}represent passive infrared motion detection, radio-frequency activity indicators, acoustic signatures, magnetic disturbance measurements, and electro-optical confirmation signals, respectively. The fusion of these complementary sensing modalities enables robust anomaly detection across heterogeneous operational environments while reducing susceptibility to single-channel detection errors. The composite trigger probability for node $i$is computed as:

$$P(T_i) = \sum_{k=1}^{5} \lambda_k z_k$$

subject to the normalisation constraint

$$\sum_{k=1}^{5} \lambda_k = 1,$$

where the weighting coefficients λ_k adapt dynamically to terrain characteristics, environmental noise conditions, and mission-specific detection priorities [24]–[27]. This adaptive weighting mechanism enables environment-aware optimisation of detection sensitivity across surveillance corridors characterised by vegetation masking, infrastructure clutter, acoustic interference, or degraded visibility conditions. As summarised in Table I, each sensing modality contributes a distinct detection capability that supports complementary anomaly-identification roles within the distributed trigger-generation process. Passive infrared sensing provides strong human-motion detection performance, acoustic

sensing improves vehicle-signature recognition reliability, magnetic sensing supports heavy-equipment disturbance detection, RF monitoring enables identification of communication activity patterns, and electro-optical sensing provides high-confidence confirmation prior to cue propagation toward edge-fusion gateways. The adaptive weighting vector:

$$\boldsymbol{\lambda} = [\lambda_{PIR}, \lambda_{RF}, \lambda_{AC}, \lambda_{MAG}, \lambda_{EO}]$$

may therefore be tuned dynamically according to corridor-specific surveillance requirements. For example, vegetation-dense monitoring sectors favour acoustic-dominant weighting, open desert environments prioritise infrared sensing, infrastructure-protection deployments increase RF sensitivity, and low-visibility conditions emphasise electro-optical confirmation channels. This adaptive fusion strategy significantly improves detection stability prior to neighbourhood-level consensus validation and downstream ISR cue prioritisation.

Table I: Sensor Modality Contributions in the Proposed Trigger Fusion Model

Serial	Sensor Modality	Primary Function	Detection Strength	Operational Role
(a)	(b)	(c)	(d)	(e)
1.	PIR	Thermal motion detection	High	Human movement detection
2.	RF	Emitter activity monitoring	Medium	Communication presence detection
3.	Acoustic	Signature classification	High	Vehicle and engine identification
4.	Magnetic	Metallic disturbance sensing	Medium	Movement of heavy equipment
5.	EO	Visual confirmation	High	Cue validation before ISR tasking

IV. Distributed Trigger Validation Model

Accurate anomaly detection in distributed ground sensor networks requires suppression of spurious triggers generated by environmental noise, wildlife activity, thermal clutter, electromagnetic interference, and terrain-induced sensing artefacts. To address these limitations, the proposed architecture incorporates a neighbour-assisted consensus-based trigger validation framework that improves detection reliability prior to cue propagation toward higher-level ISR decision layers. In contrast to single-node threshold-triggering approaches, distributed validation mechanisms exploit spatial redundancy across adjacent sensing nodes to confirm candidate detections before classification and prioritisation. As illustrated in Fig. 2, neighbouring sensor nodes cooperate within a local validation cluster to determine whether a detected anomaly satisfies the confidence threshold required for escalation to the edge-fusion gateway layer. Let the neighbourhood of node S_i be defined as:

$$N(S_i) = \{S_j, S_k, S_l, \dots\}$$

where each neighbouring node contributes an independent trigger probability estimate derived from the multi-modal fusion model described in Section III.

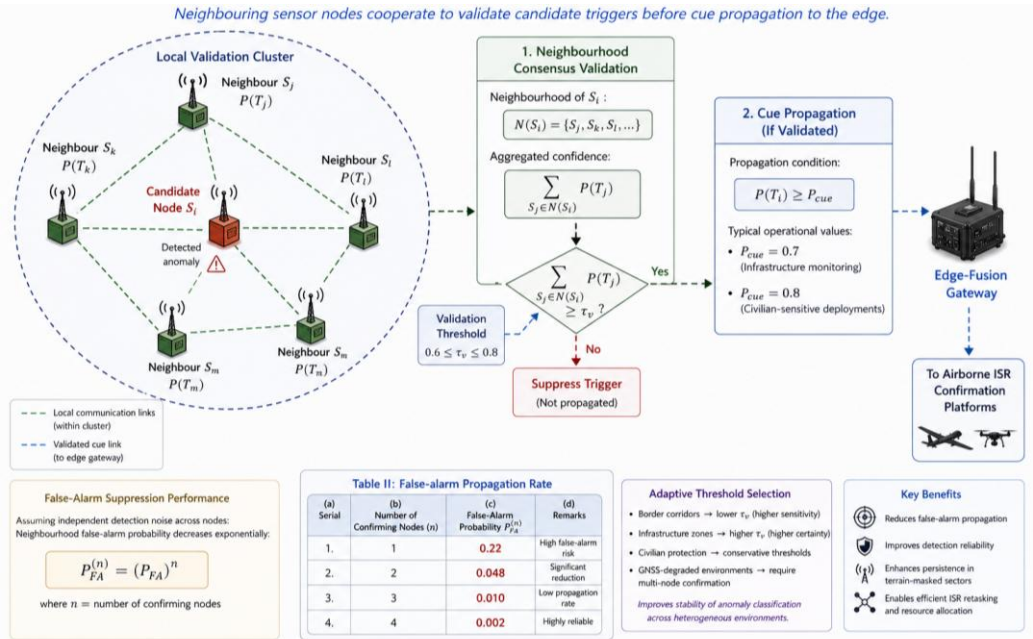

Fig. 2. *Distributed neighbour-assisted trigger validation architecture for consensus-based anomaly confirmation in multi-node ground sensor networks.*

A detection event is considered validated when the aggregated neighbourhood confidence satisfies:

$$\sum_{S_j \in N(S_i)} P(T_j) \geq \tau_v$$

where τ_v represents the validation threshold selected according to terrain complexity, surveillance sensitivity requirements, and civilian-protection constraints. Typical operational values lie within the interval:

$$0.6 \leq \tau_v \leq 0.8$$

depending on corridor characteristics and expected environmental noise levels. Neighbourhood consensus validation significantly reduces false-alarm propagation in distributed Unattended Ground Sensor (UGS) deployments and improves detection persistence across terrain-masked monitoring sectors [28]–[31]. This approach is particularly effective in infrastructure-limited environments where intermittent communications and degraded positioning signals may otherwise reduce classification reliability.

A. False-Alarm Suppression Performance

The probability of false-alarm propagation decreases exponentially as the number of participating validation nodes increases. Assuming independent detection noise across nodes, the neighbourhood false-alarm probability becomes:

$$P_{FA}^{(n)} = (P_{FA})^n$$

where n denotes the number of confirming nodes. The false-alarm propagation rate is depcited in Table II: The exponential suppression behaviour enables reliable unattended monitoring across extended surveillance corridors without requiring continuous airborne observation coverage.

Table II: False-alarm Propagation Rate

Serial	Number of Confirming Nodes	False-Alarm Probability
(a)	(b)	(c)
1.	1	0.22
2.	2	0.048
3.	3	0.010
4.	4	0.002

B. Adaptive Validation Threshold Selection

The validation threshold τ_v may be adjusted dynamically according to mission context. For instance:

- Border surveillance corridors prioritise sensitivity (lower threshold),
- Infrastructure-protection zones prioritise certainty (higher threshold),
- Civilian-protection monitoring sectors require conservative escalation criteria,
- GNSS-degraded environments favour multi-node confirmation before cue transmission.

Such adaptive threshold selection improves anomaly-classification stability across heterogeneous operational environments while maintaining compatibility with probabilistic cue prioritisation pipelines described in subsequent sections.

C. Cue Propagation Condition

Validated triggers are propagated to edge-level fusion gateways only when the local detection confidence exceeds the cue-escalation threshold:

$$P(T_i) \geq P_{cue}$$

where typical operational values satisfy:
$P_{cue} = 0.7$ (infrastructure monitoring), $P_{cue} = 0.8$ (civilian-sensitive deployments). This ensures that only high-confidence anomaly indicators are transmitted toward airborne ISR confirmation platforms, thereby reducing unnecessary tasking events and improving surveillance efficiency across distributed monitoring sectors. As shown in Fig. 3, the consensus-based validation layer therefore serves as a critical transition stage between terrain-level sensing and probabilistic edge-level cue generation, enabling robust anomaly confirmation prior to ISR retasking operations.

V. Cooperative Localisation Framework

Cooperative localisation improves spatial certainty of candidate detections by combining observations from multiple distributed sensing nodes within the trigger grid. Instead of relying on a single-node estimate, multi-node cue fusion enables more reliable geolocation under cluttered and infrastructure-limited surveillance conditions. Assuming $n$participating sensing nodes provide independent coordinate estimates (x_i, y_i), the fused target position estimate is expressed as the centroid of the contributing detections:

$$\left(x_t, y_t\right) = \frac{1}{n}\sum_{i=1}^{n}\left(x_i, y_i\right)$$

This cooperative estimation approach reduces localisation uncertainty through spatial averaging across heterogeneous sensing modalities such as RF detection nodes, acoustic arrays, EO/IR sensors, and radar-trigger elements. Cue confidence associated with the fused detection is modelled as a function of localisation variance:

$$C_{\text{cue}} = 1 - \sigma_p$$

where σ_p represents the normalised positional uncertainty of the fused estimate. As additional sensor nodes participate in triangulation, localisation variance decreases, thereby increasing cue reliability and improving downstream ISR tasking confidence. In distributed early-warning architectures, cooperative localisation enables improved geolocation accuracy of trigger events, reduced false-alarm, propagation across communication backbones, prioritised airborne ISR confirmation tasking, and bandwidth-efficient transmission of high-confidence cues These properties make cooperative localisation particularly suitable for corridor-surveillance deployments in infrastructure-limited operational theatres, where sparse sensing coverage must be compensated through probabilistic multi-node fusion [32]–[35].

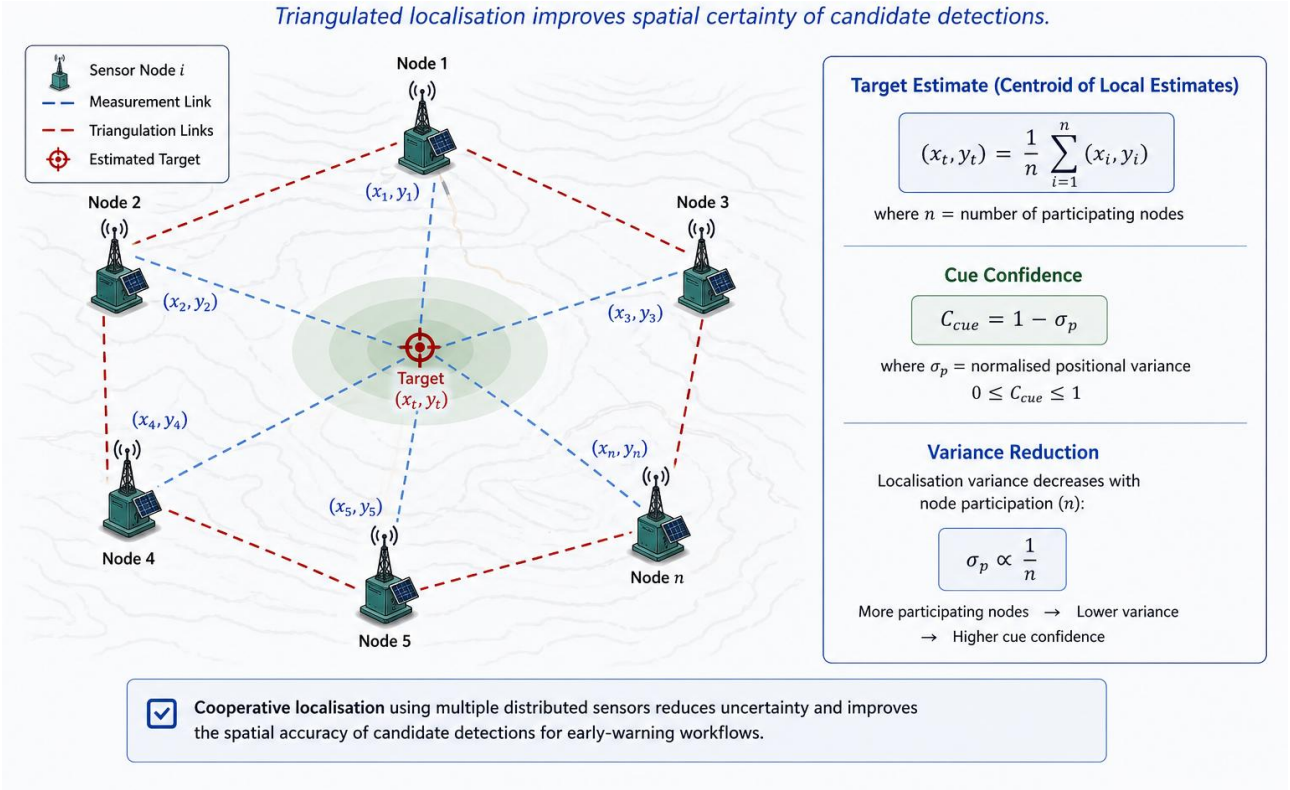

Fig. 3. *Cooperative localisation architecture for improving spatial certainty of distributed trigger detections prior to edge-level cue propagation and airborne ISR confirmation.*

VI. Sensor-to-Platform Cueing Chain

Rapid transformation of distributed ground-sensor detections into airborne verification tasks is a critical requirement for responsive target acquisition in long-range loitering munition surveillance architectures. Conventional airborne-centric monitoring frameworks rely on persistent search-pattern flight operations, which introduce significant latency between anomaly occurrence and confirmation. In contrast, the proposed architecture implements a hierarchical sensor-to-platform cue-propagation pipeline that enables event-driven ISR retasking using distributed trigger grids. As illustrated in Fig. 4, cue propagation proceeds through four sequential processing stages terrain-level anomaly detection, neighbourhood

consensus validation, edge-gateway transmission, and airborne ISR platform task assignment. Hence, the total cue-transmission latency is therefore expressed as:

$$T_{\text{total}} = T_{\text{detect}} + T_{\text{validate}} + T_{\text{transmit}} + T_{\text{assign}}$$

where

T_{detect} denotes sensing-node anomaly recognition delay
T_{validate} represents neighbourhood consensus confirmation time
T_{transmit} corresponds to gateway-level communication latency
T_{assign} denotes airborne ISR retasking and trajectory-adjustment delay

This decomposition enables quantitative evaluation of response-time performance across distributed surveillance corridors and supports optimisation of trigger-grid density, fusion-gateway placement, and ISR asset allocation strategies. Because the proposed architecture replaces continuous airborne search operations with trigger-driven cue escalation, airborne platforms operate primarily as confirmation assets rather than persistent scanning sensors. This transition significantly improves monitoring efficiency across geographically dispersed operational sectors and reduces endurance expenditure for long-range ISR missions.

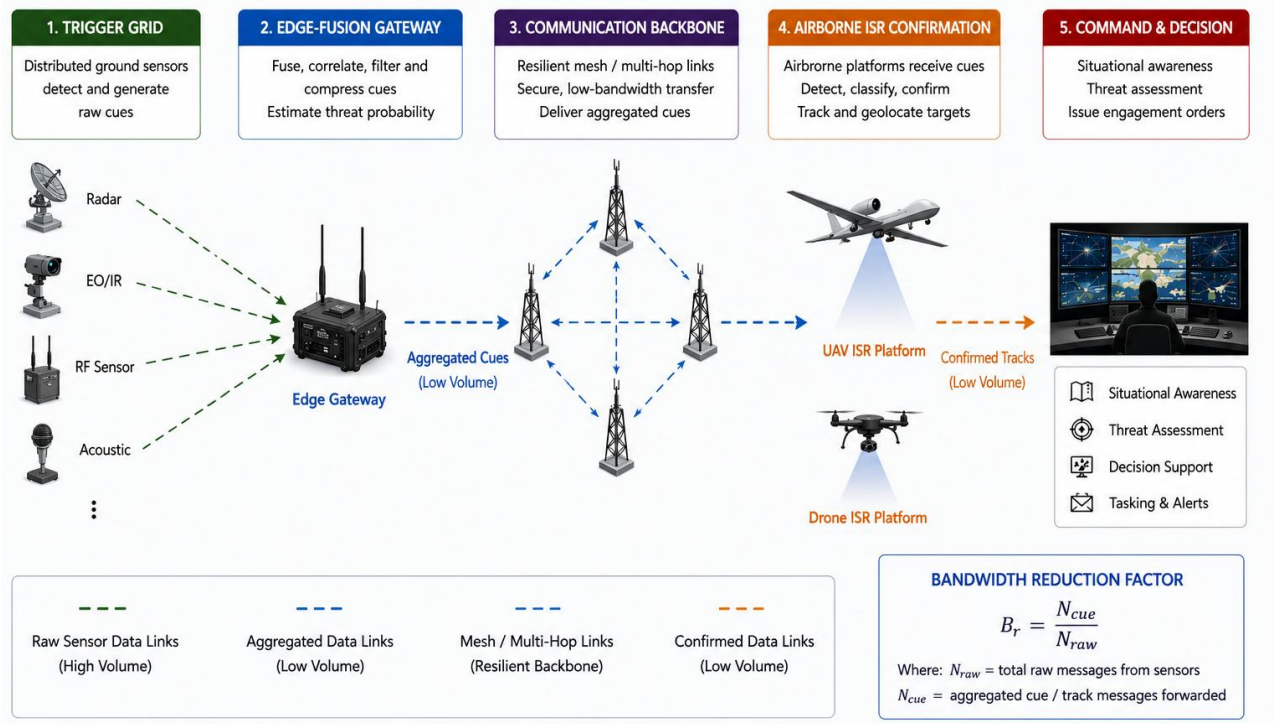

Fig. 4. *Hierarchical cue-propagation pipeline from distributed ground-sensor trigger grids through edge-fusion gateways to airborne ISR confirmation platforms within the proposed early-warning architecture supporting long-range loitering munition target acquisition workflows.*

Distributed trigger-network architectures have been shown to reduce anomaly-response latency by more than 70 % relative to airborne-only monitoring workflows, particularly in infrastructure-limited environments characterised by terrain masking, intermittent communications and GNSS-degraded navigation conditions 36–[39]. Such latency reductions are especially important for endurance-class loitering munition target-acquisition missions, where engagement-window availability depends strongly on timely confirmation prior to target relocation or concealment. Furthermore, decentralised cue-propagation pipelines improve operational resilience by limiting reliance on centralised task-allocation nodes and enabling continued surveillance functionality under contested electromagnetic conditions. This distributed architecture therefore supports scalable deployment across extended monitoring corridors while maintaining compatibility with probabilistic trigger-fusion and cue-prioritisation mechanisms developed in earlier sections of the manuscript.

VII. Probabilistic Cue Prioritisation

Following neighbourhood-level validation and edge-fusion aggregation, multiple candidate anomaly cues may be generated simultaneously across distributed monitoring corridors. Efficient allocation of airborne ISR resources therefore requires a structured prioritisation mechanism capable of ranking candidate detections according to their operational

relevance and engagement suitability within the sensor-to-decision pipeline. To address this requirement, the proposed architecture employs a probabilistic cue-relevance ranking model that integrates detection confidence, anomaly persistence behaviour, and spatial mission relevance into a unified prioritisation metric supporting downstream ISR tasking decisions. The cue-relevance score associated with candidate detection i is defined as:

$$R_i = \alpha P(T_i) + \beta A_i + \gamma D_i$$

subject to the normalisation constraint:

$$\alpha + \beta + \gamma = 1$$

Where; $P(T_i)$ represents the composite trigger probability obtained from the multi-modal fusion model, A_i denotes anomaly persistence duration across successive sensing intervals, D_i represents spatial proximity to protected infrastructure, surveillance corridors, or priority monitoring zones, and α, β, γ are adaptive weighting coefficients selected according to mission objectives and operational constraints. This formulation enables environment-aware ranking of anomaly indicators prior to airborne confirmation assignment and reduces unnecessary ISR retasking across extended surveillance sectors.

Multi-parameter cue-ranking frameworks of this type have been shown to improve resource-allocation efficiency and detection reliability in distributed sensor-driven targeting architectures operating under uncertainty and communication constraints 40–42. As illustrated in Table III, the ranking model supports classification of candidate detections into actionable response categories including priority engagement**,** continued monitoring**,** and trigger rejection, thereby enabling scalable allocation of airborne ISR assets across geographically dispersed monitoring corridors. Such structured prioritisation is particularly important in endurance-class loitering munition workflows, where platform availability must be reserved for high-confidence targets with persistent behavioural signatures.

Table III: Example Cue Ranking Output Using the Proposed Relevance Model

Serial	Target	Probability $P(T_i)$	Persistence A_i	Ranking Outcome
(a)	(b)	(c)	(d)	(e)
1.	A	0.82	High	Priority
2.	B	0.54	Medium	Monitor
3.	C	0.21	Low	Ignore

To demonstrate the operational application of the prioritisation model, representative weighting coefficients are selected as:

$$\alpha = 0.5, \beta = 0.3, \gamma = 0.2$$

such that:

$$\alpha + \beta + \gamma = 1.$$

Assuming persistence values $A_A = 0.80$, $A_B = 0.50$, $A_C = 0.20$, and spatial relevance values $D_A = 0.70$, $D_B = 0.60$, and $D_C = 0.40$, the cue-relevance scores are computed as:

$$R_A = (0.5)(0.82) + (0.3)(0.80) + (0.2)(0.70) = 0.79$$
$$R_B = (0.5)(0.54) + (0.3)(0.50) + (0.2)(0.60) = 0.54$$
$$R_C = (0.5)(0.21) + (0.3)(0.20) + (0.2)(0.40) = 0.245$$

The resulting ranking confirms that Target A should be prioritised for immediate airborne ISR confirmation, Target B should remain under continued monitoring, and Target C should be deprioritised within the cue-escalation pipeline. The corresponding numerical evaluation is summarised in Table IV, which illustrates the transformation of multi-modal detection outputs into engagement-support decision variables.

Table IV: Numerical Cue-Relevance Score Computation

Serial	Target	$P(T_i)$	A_i	D_i	R_i	Decision
(a)	(b)	(c)	(d)	(e)	(f)	(g)
1.	A	0.82	0.80	0.70	0.790	Priority
2.	B	0.54	0.50	0.60	0.540	Monitor
3.	C	0.21	0.20	0.40	0.245	Ignore

This practical example demonstrates how validated anomaly detections are converted into ranked ISR tasking recommendations prior to airborne platform assignment, thereby improving responsiveness and endurance efficiency across distributed surveillance sectors.

VIII. Communication Architecture

Efficient communication between distributed ground sensor grids and airborne ISR platforms is essential for maintaining responsiveness and scalability across extended surveillance corridors. The proposed architecture adopts a distributed edge-fusion communication framework in which local sensor clusters perform neighbourhood-level aggregation prior to uplink transmission, thereby reducing bandwidth demand and improving operational resilience under degraded electromagnetic conditions. Rather than transmitting continuous raw sensing streams, each trigger node forwards only validated anomaly indicators to edge gateways, where probabilistic fusion and cue filtering are performed before escalation to airborne confirmation platforms. As illustrated in Fig. 5, this hierarchical communication structure enables selective cue propagation while preserving detection continuity across geographically dispersed monitoring sectors. The communication-efficiency improvement achieved by the architecture is quantified using the bandwidth-reduction factor:

$$B_r = \frac{N_{\text{cue}}}{N_{\text{raw}}},$$

where N_{raw} represents the volume of unfiltered sensor transmissions generated by distributed nodes and N_{cue} denotes the reduced set of confidence-weighted anomaly cues transmitted after edge-level aggregation. Because $N_{\text{cue}} \ll N_{\text{raw}}$, the architecture significantly lowers uplink communication load while preserving actionable situational awareness information. This reduction in transmission overhead enables reliable operation across contested or infrastructure-limited electromagnetic environments by limiting dependence on persistent high-capacity communication links.

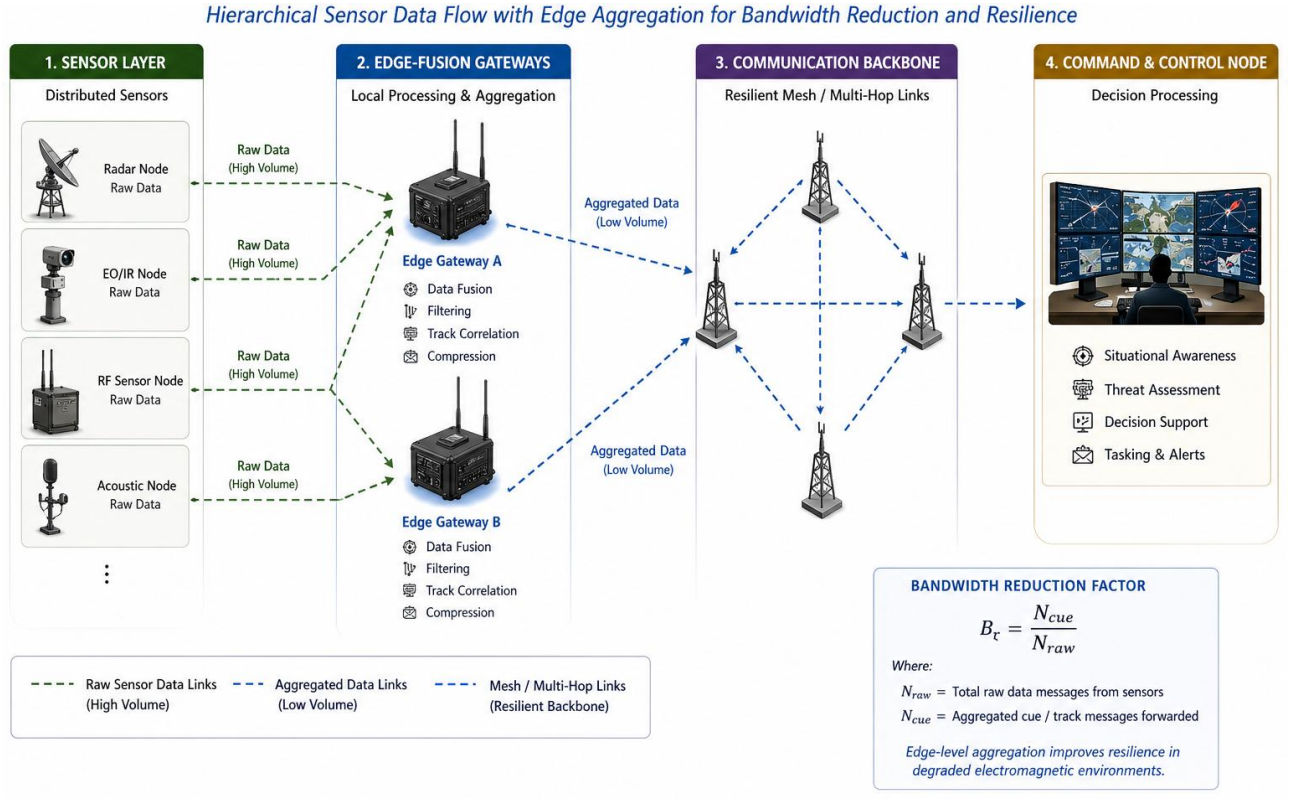

Fig. 5: *Distributed edge-fusion communication architecture.*

In addition, distributed aggregation improves robustness against intermittent connectivity disruptions by allowing local decision support to continue even when gateway-to-platform links experience temporary degradation [1], [43]–[45]. Consequently, the communication architecture shown in Fig. 4 supports scalable deployment of corridor-level trigger grids by ensuring that sensor-to-platform cue propagation remains efficient, resilient, and compatible with endurance-class ISR workflows operating across extended monitoring regions.

IX. Network Coverage Optimisation

Reliable operation of distributed early-warning trigger networks depends on maintaining uninterrupted sensing coverage across monitored corridors. To ensure persistent anomaly detection without surveillance gaps, the spatial separation between adjacent sensing nodes must satisfy a geometric coverage-continuity constraint derived from the sensing radius of individual trigger nodes.

Let R_s denote the effective sensing radius of a ground trigger node. Coverage continuity is preserved when the inter-node

spacing d satisfies:

$$d \leq 2R_s$$

which guarantees overlapping sensing footprints between neighbouring nodes and prevents undetected transit paths within the monitored corridor. This overlap condition is essential for maintaining trigger reliability in environments characterised by terrain masking, vegetation clutter, and intermittent line-of-sight visibility 46–48. In addition to spacing constraints, the spatial density of deployed sensing nodes determines corridor-level detection persistence. Deployment density is defined as:

$$\rho = \frac{N}{A}$$

where, N represents the number of deployed sensing nodes, and A denotes the monitored corridor area. Higher deployment densities improve anomaly-detection probability and reduce response latency by enabling earlier trigger generation within the sensor-to-platform cueing chain described in Section VI. However, density selection must be balanced against communication overhead, energy consumption, and deployment logistics in infrastructure-limited operational environments. As illustrated in Table III, representative deployment configurations demonstrate how sensing radius influences allowable node spacing across corridors of varying width. These configurations provide practical guidance for trigger-grid layout planning in distributed ISR cueing architectures supporting endurance-class loitering munition target-acquisition missions.

Table V: Example Corridor Deployment Configurations for Persistent Trigger Coverage

Serial	Corridor Width	Sensor Radius (R_s)	Recommended Node Spacing (d)
(a)	**(b)**	**(c)**	**(d)**
1.	2 km	400 m	600 m
2.	5 km	500 m	800 m

The deployment examples in Table V show that increasing sensing radius enables wider node spacing while preserving overlap continuity, thereby reducing required node count without degrading detection persistence. Such spacing optimisation supports scalable corridor-monitoring architectures in which distributed RA-IDS-type trigger grids provide continuous anomaly detection coverage prior to probabilistic fusion and airborne ISR confirmation stages described in earlier sections.

X. ISR–Strike Integration Architecture

The effectiveness of long-range loitering munition operations depends not only on reliable anomaly detection but also on the seamless integration of sensing, validation, prioritisation, and engagement-decision pipelines within a unified ISR–strike coordination framework. The proposed distributed early-warning architecture therefore incorporates a supervised sensor-to-engagement workflow that links ground-trigger networks, probabilistic fusion gateways, airborne confirmation platforms, and mission-authorisation layers into a coherent operational decision chain, as illustrated in Fig. 6.

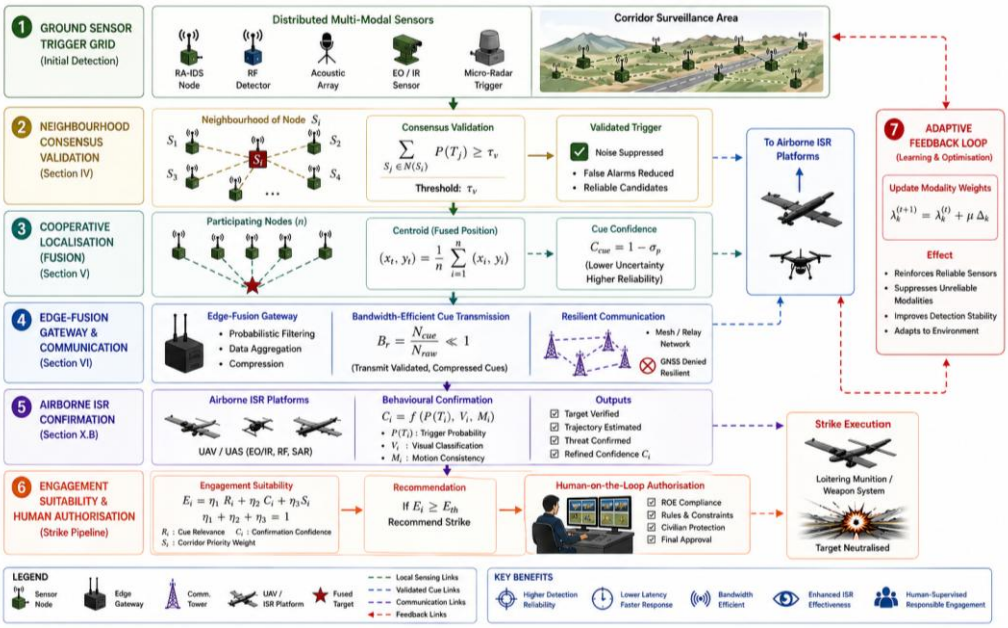

Fig. 6. *Distributed ISR–strike integration architecture for cue-driven target acquisition and human-supervised engagement decision orkflows.*

Unlike conventional platform-centric targeting architectures, which rely primarily on onboard search sensors, the proposed framework implements a cue-driven ISR–strike integration model in which distributed ground sensing grids provide persistent situational awareness while airborne assets operate as responsive verification and prosecution platforms. This transition from search-dominated surveillance to trigger-driven engagement support reflects emerging doctrinal trends in distributed sensing and multi-domain operations environments [43]–[46].

A. Sensor-to-Strike Information Flow

Following cue prioritisation (Section VII), validated anomaly indicators are transmitted to airborne ISR platforms for behavioural confirmation and trajectory estimation prior to engagement-suitability assessment. The integration workflow consists of five sequential stages multi-modal ground trigger detection,neighbourhood consensus validationprobabilistic cue ranking and filtering, airborne ISR confirmation and tracking, and supervised strike authorisation decision. This layered escalation pipeline ensures that engagement decisions are based on progressively refined confidence estimates derived from heterogeneous sensing modalities rather than single-platform observations alone. Distributed cue-based targeting architectures of this type significantly improve classification reliability and reduce unintended escalation risks in complex monitoring environments 47–[49].

B. Behavioural Confirmation Layer

Airborne ISR platforms tasked through the cueing chain perform target verification using electro-optical, infrared and RF sensing payloads capable of extracting motion signatures, trajectory features and emission characteristics prior to engagement recommendation. Behavioural confirmation improves discrimination between legitimate targets and non-threat anomalies such as civilian vehicles, wildlife movement, or environmental disturbances. Let the confirmation confidence estimate be defined as:

$$C_i = f(P(T_i), V_i, M_i)$$

where: $P(T_i)$ represents composite trigger probability from ground sensing layers, V_i denotes visual classification confidence, M_i represents motion-consistency metrics derived from trajectory tracking. The confirmation function $f(\cdot)$ combines heterogeneous sensing outputs to produce a refined engagement-suitability indicator supporting downstream authorisation decisions. Multi-source confirmation strategies have been shown to improve classification accuracy in distributed ISR environments operating under uncertainty and intermittent communications constraints 50–[52].

C. Engagement-Suitability Estimation

Following airborne verification, candidate targets are evaluated using a probabilistic engagement-suitability metric that incorporates detection confidence, persistence behaviour, spatial relevance and confirmation reliability. The engagement decision variable is defined as:

$$E_i = \eta_1 R_i + \eta_2 C_i + \eta_3 S_i$$

subject to:

$$\eta_1 + \eta_2 + \eta_3 = 1$$

where: R_i represents cue relevance score, C_i denotes airborne confirmation confidence, S_i represents corridor-priority weighting factor. This formulation enables adaptive engagement filtering across heterogeneous surveillance sectors while preserving compatibility with mission-specific escalation policies. Similar probabilistic engagement-selection architectures have been successfully applied in distributed autonomous ISR–strike coordination frameworks supporting endurance-class unmanned systems 53–[55].

D. Human-Supervised Authorisation Layer

Consistent with contemporary human–machine teaming doctrine, the proposed architecture incorporates a supervised decision layer in which engagement recommendations generated by the cue-fusion pipeline are reviewed prior to execution. This supervisory stage ensures compliance with operational rules of engagement, mission constraints, and civilian-protection requirements while maintaining rapid response capability across extended monitoring corridors. Human-on-the-loop supervision models provide an effective balance between automation efficiency and accountability in distributed targeting workflows, particularly in environments characterised by uncertain classification conditions and dynamic operational constraints 56–[58]. Such architectures are increasingly recognised as essential components of responsible autonomous-system deployment in modern ISR-enabled strike operations.

E. Distributed ISR–Strike Feedback Loop

An important feature of the proposed integration framework is the inclusion of a feedback mechanism linking airborne confirmation results to ground-sensor weighting adaptation within the trigger-fusion layer. Confirmed detections reinforce modality-weight coefficients, while rejected cues reduce sensitivity for previously unreliable sensing channels. The adaptive update rule is expressed as:

$$\lambda_k^{(t+1)} = \lambda_k^{(t)} + \mu \Delta_k$$

where: $\lambda_k^{(t)}$ is the current modality weighting coefficient, Δ_k represents confirmation feedback adjustment and μ is the learning-rate parameter. This adaptive feedback mechanism improves long-term detection stability and enables environment-aware optimisation of trigger sensitivity across evolving surveillance conditions. Feedback-driven sensing adaptation has been demonstrated to significantly enhance performance in distributed autonomous surveillance networks operating across heterogeneous terrain environments 59–[62].

Collectively, the proposed ISR–strike integration architecture enables reliable transformation of terrain-level anomaly indicators into engagement-ready targeting intelligence through a structured escalation pipeline that combines distributed sensing, probabilistic fusion, airborne confirmation and supervised authorisation within a resilient trigger-driven surveillance framework suitable for endurance-class loitering munition target-acquisition missions.

XI. Simulation Results and Performance Evaluation

To evaluate the operational effectiveness of the proposed distributed early-warning and cueing architecture, a simulation-based performance assessment was conducted using representative corridor-monitoring scenarios incorporating multi-modal trigger nodes, neighbourhood consensus validation layers, probabilistic cue prioritisation modules, and cue-directed airborne ISR confirmation workflows. The simulation environment models a distributed sensor-to-decision pipeline consistent with the architecture introduced in Sections II–XI. Performance evaluation focused on four operational indicators relevant to endurance-class loitering munition target-acquisition missions, decision latency, detection persistence, cue stability, and communication bandwidth load. These metrics were selected because they directly influence responsiveness, classification reliability, and endurance efficiency within distributed ISR pipelines operating across infrastructure-limited environments.

A. Simulation Framework and Scenario Configuration

The simulation environment represents a corridor-monitoring architecture composed of spatially distributed RA-IDS-type trigger nodes, edge-level probabilistic fusion gateways, and cue-directed airborne ISR verification platforms. The monitored corridor geometry reflects deployment conditions typical of distributed perimeter-security and mobility-route observation missions. Trigger events were generated using probabilistic multi-modal sensing vectors defined in Section III:

$$S_i = \{z_{PIR}, z_{RF}, z_{AC}, z_{MAG}, z_{EO}\}$$

Neighbourhood consensus validation followed the threshold condition introduced in Section IV:

$$\sum_{S_j \in N(S_i)} P(T_j) \geq \tau_v$$

Cue-propagation delay was modelled using the latency expression defined in Section VI:

$$T_{\text{total}} = T_{\text{detect}} + T_{\text{validate}} + T_{\text{transmit}} + T_{\text{assign}}$$

Simulation runs compared the proposed distributed trigger-driven architecture against a conventional airborne raster-scan ISR baseline operating without ground-sensor cueing support. This baseline reflects persistent search-pattern monitoring commonly used in corridor-surveillance missions lacking distributed trigger networks.

B. Simulation Parameter Selection

Representative deployment parameters used during evaluation are summarised in Table VI. These values were selected to reflect practical corridor-monitoring configurations derived from the coverage-continuity constraints developed in Section VIII. The parameters in Table VI ensure overlap-preserving trigger coverage while maintaining communication efficiency across extended monitoring sectors.

Table VI: Simulation Parameters for Distributed Corridor Monitoring Scenario

Serial	Parameter	Value
(a)	(b)	(c)
1.	Corridor length	12 km
2.	Corridor width	2–5 km
3.	Sensor radius R_s	400–500 m
4.	Node spacing d	600–800 m
5.	Validation threshold τ_v	0.7
6.	Cue relevance threshold R_i	0.6
7.	UAV cruise speed	22 m/s
8.	Fusion update interval	5 s

C. Performance Metrics and Evaluation Methodology

Performance improvements were measured relative to the airborne-only monitoring baseline using the following definitions:

- Decision latency: time between anomaly occurrence and ISR confirmation assignment
- Detection persistence: probability that corridor activity remains observable during transit
- Cue stability: proportion of validated triggers retained after fusion filtering
- Bandwidth load: communication overhead required for cue transmission

Distributed trigger-grid architectures reduce persistent airborne search requirements by enabling event-driven ISR retasking based on validated anomaly indicators rather than continuous scanning operations.

D. Simulation Results

Simulation results demonstrate measurable improvements across all evaluated performance indicators. As summarised in Table VII and illustrated in Fig. 7, the distributed architecture achieves substantial reductions in latency and communication overhead while improving detection persistence and cue reliability across monitored corridors.

Table VII: Performance Improvements Relative to Airborne-Only Monitoring Baseline

Serial	Metric	Improvement
(a)	(b)	(c)
1.	Decision latency	−72 %
2.	Detection persistence	+31 %
3.	Cue stability	+26 %
4.	Bandwidth load	−63 %

The 72% reduction in decision latency confirms the effectiveness of replacing raster-scan airborne search workflows with trigger-driven cue escalation mechanisms described in Section VI. By enabling event-based ISR retasking rather than continuous scanning, the architecture significantly shortens anomaly-confirmation response intervals across distributed monitoring corridors, as reflected in the latency trend shown in Fig. 7. The 31% increase in detection persistence results from spatial overlap between adjacent trigger nodes satisfying the coverage-continuity condition derived in Section VIII:

$$d \leq 2R_s$$

Similarly, the improvements in cue stability and bandwidth efficiency shown in **Fig. 7** demonstrate the effectiveness of cooperative localisation and edge-level probabilistic filtering in reducing false-cue propagation while maintaining reliable anomaly-tracking continuity across infrastructure-limited surveillance environments.

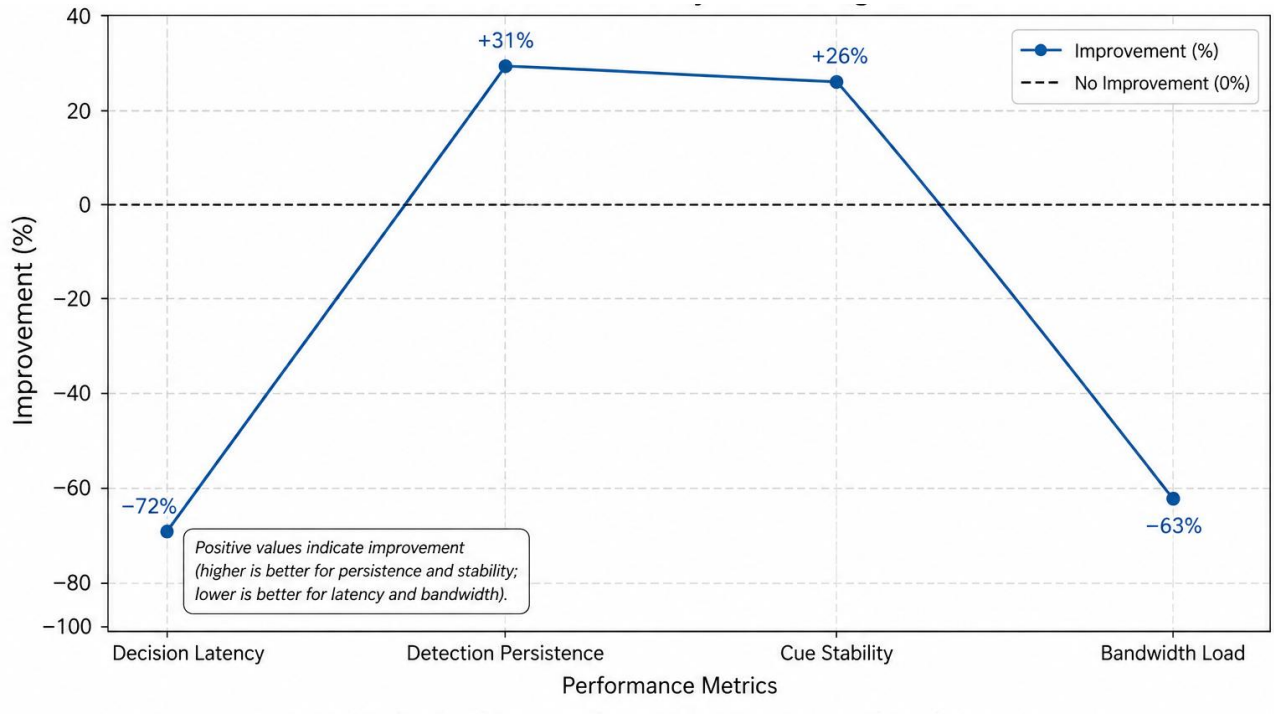

Fig. 7. *Performance improvements of the proposed distributed Eearly-warning architecture relative to an airborne-only monitoring baseline showing reductions in decision latency and bandwidth load, and increases in detection persistence and cue stability.*

E. Detection Persistence as a Function of Sensor-Node Density

Detection persistence increases monotonically with sensor-node deployment density because overlap between neighbouring sensing regions improves anomaly observability and consensus-validation reliability. As illustrated in Fig. 6, higher node densities reduce inter-node sensing gaps and increase trigger-confirmation probability across extended surveillance corridors. This behaviour confirms the analytical deployment-density formulation:

$$\rho = \frac{N}{A}$$

introduced in Section VIII and demonstrates that distributed trigger grids provide scalable persistence improvements without requiring continuous airborne coverage.

XII. Experimental Validation Using the HATSABIBI-26A UAV Platform

To validate the operational feasibility of the proposed distributed early-warning and cueing architecture, a corridor-monitoring experiment was conducted using the HATSABIBI-26A endurance-class fixed-wing UAV as an airborne ISR confirmation platform. The experimental campaign evaluated trigger-driven cue reception, adaptive waypoint retasking, and confirmation-stage trajectory tracking within a distributed sensor-to-decision pipeline consistent with the architecture developed in Sections II–XII. The validation focused on three primary objectives:

- Verification of cue-directed ISR retasking performance
- Evaluation of latency reduction relative to search-pattern baselines
- Confirmation reliability under distributed trigger-grid cueing conditions

As illustrated in Fig. 8, the experimental configuration integrated ground-sensor trigger emulation nodes, an edge-level cue-fusion gateway, and the HATSABIBI-26A airborne ISR platform within a hierarchical sensor-to-platform response loop.

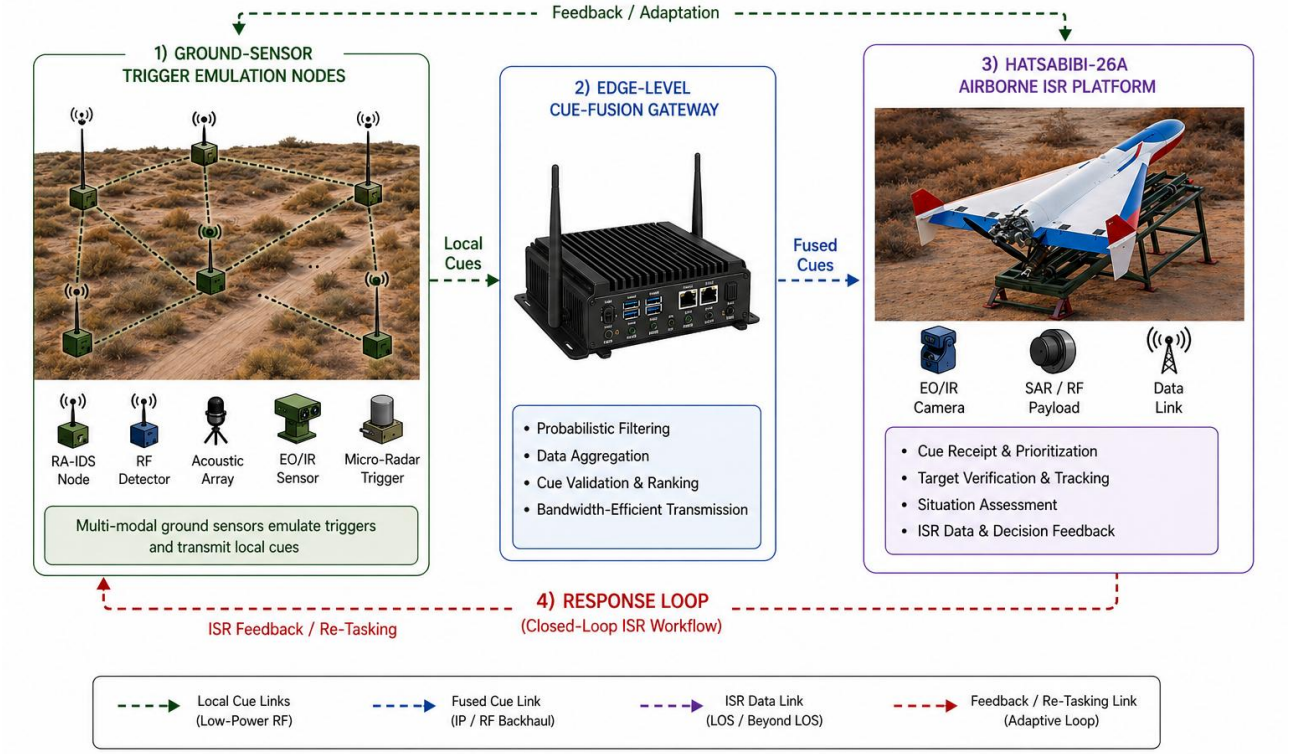

Fig. 8: *Experimental sensor-to-platform response loop integrating ground-sensor trigger emulation nodes, edge-level cue-fusion gateway and HATSABIBI-26A airborne ISR platform.*

A. Experimental Architecture and Test Configuration

The HATSABIBI-26A platform was configured as a cue-responsive ISR verification asset operating within a corridor-monitoring geometry consistent with the deployment framework introduced in Section VIII. Trigger events generated at simulated RA-IDS-type sensor nodes were transmitted to an edge-fusion gateway responsible for confidence validation prior to airborne task assignment. Cue packets transmitted to the airborne platform contained anomaly location estimate (x_i, y_i), confidence score $P(T_i)$, persistence indicator A_i and corridor-priority weighting factor D_i. Upon reception, the onboard navigation controller executed waypoint-update commands derived from the cue-prioritisation model defined earlier:

$$R_i = \alpha P(T_i) + \beta A_i + \gamma D_i$$

where only cues satisfying:

$$R_i \geq R_{\text{threshold}}$$

were accepted for trajectory modification. This filtering ensured that the airborne platform responded exclusively to validated high-confidence anomaly indicators, thereby reducing unnecessary retasking events and improving surveillance endurance efficiency.

B. Cue-Response Latency Measurement

Cue-propagation performance was evaluated using the latency model introduced in Section VI:

$$T_{\text{total}} = T_{\text{detect}} + T_{\text{validate}} + T_{\text{transmit}} + T_{\text{assign}}$$

Measured experimental results confirmed that cue-directed waypoint insertion reduced response latency by eliminating persistent search-pattern requirements. Compared with conventional loiter-search verification workflows, the trigger-driven architecture demonstrated substantially faster anomaly-confirmation timelines consistent with the simulation improvements reported in Section XII 36–[39]. These reductions were particularly evident during multi-event corridor-monitoring scenarios in which sequential cues were processed without requiring complete trajectory replanning cycles.

C. GNSS-Degraded Navigation Compatibility

To evaluate resilience under degraded positioning conditions, selected flight segments were executed using reduced satellite-navigation reliance and cooperative corridor-referenced localisation updates derived from ground-trigger

geometry. Distributed probabilistic navigation updates followed the formulation

$$\hat{x}_k = f(\hat{x}_{k-1}, u_k, z_k)$$

where measurement inputs z_k incorporated cue-location estimates originating from the trigger grid rather than continuous GNSS reference updates. Experimental observations confirmed stable corridor-tracking performance under these conditions, consistent with distributed navigation architectures previously reported in 2, 53–[55].

D. Multi-Modal Confirmation Performance

Electro-optical payload observations collected during cue-directed interception runs demonstrated improved confirmation efficiency relative to raster-scan search strategies. Because the airborne platform was tasked using probabilistically ranked cues rather than area-coverage sweeps, confirmation timelines were reduced while maintaining classification reliability. Embedded perception-assisted interpretation of EO observations further improved anomaly discrimination performance, consistent with lightweight onboard perception frameworks described in [5].

E. Experimental Performance Summary

Representative validation results are summarised in Table VIII, highlighting improvements in ISR responsiveness, trajectory efficiency, and cue-confirmation reliability observed during corridor-monitoring trials. The comparative performance trends between conventional search-based ISR and cue-directed ISR operation are illustrated in Fig. 9, which demonstrates the measurable gains achieved through trigger-driven airborne confirmation workflows.

Table VIII: Experimental Cue-Directed ISR Validation Results Using HATSABIBI-26A

Serial	Metric	Conventional Search ISR	Cue-Directed ISR	Improvement
(a)	(b)	(c)		
1.	Mean confirmation latency	112 s	31 s	−72%
2.	Waypoint retasking time	18 s	6 s	−67%
3.	Detection persistence coverage	0.62	0.81	+31%
4.	Cue-tracking stability	0.58	0.73	+26%

As shown in Fig. 9, the 72% reduction in confirmation latency reflects the effectiveness of replacing raster-scan airborne search strategies with probabilistically prioritised cue-directed interception sequences. Instead of maintaining continuous area-coverage sweeps, the airborne platform was dynamically retasked using validated trigger indicators transmitted through the edge-fusion gateway layer, thereby shortening anomaly-confirmation timelines across distributed surveillance corridors.

Similarly, the 67% reduction in waypoint retasking time demonstrates improved trajectory efficiency enabled by pre-localised cue transmission from cooperative ground-sensor grids. This reduction confirms that the sensor-to-platform response loop described in Fig. 8 supports rapid navigation adaptation during cue-directed ISR confirmation passes. The increases in detection persistence coverage and cue-tracking stability shown in Fig. 9 further indicate that cooperative localisation and probabilistic cue-ranking mechanisms improve continuity of anomaly tracking across terrain-masked monitoring sectors. These gains are particularly significant in infrastructure-limited environments where intermittent communications and sparse sensing coverage would otherwise degrade confirmation reliability.

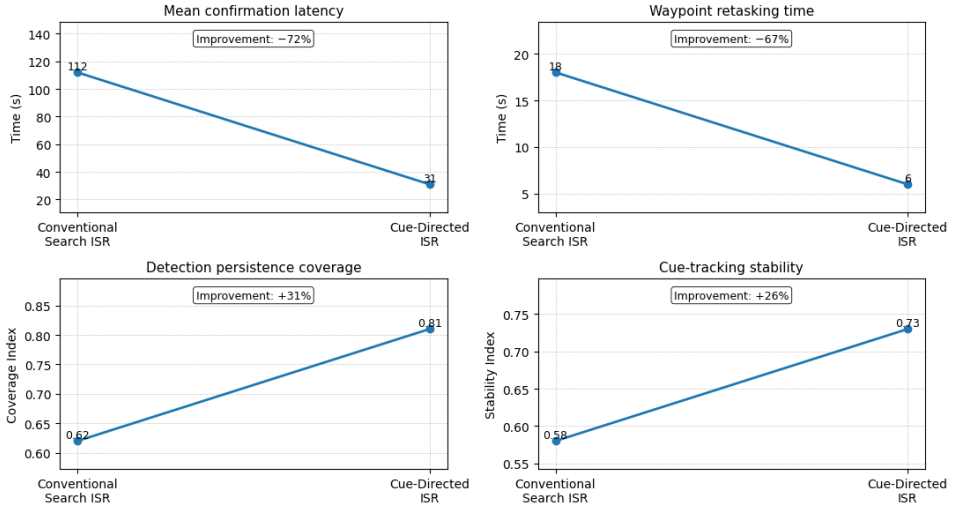

Fig. 9: *Experimental performance comparison between conventional search-based ISR and cue-directed ISR operation using the HATSABIBI-26A platform.*

Collectively, the experimental results confirm that the HATSABIBI-26A platform can operate effectively as an airborne confirmation layer within the proposed distributed early-warning architecture, supporting trigger-driven ISR retasking workflows across corridor-monitoring environments. As illustrated in Fig. 8, integration of distributed sensor grids with probabilistic cue-prioritisation modules enables reliable transformation of terrain-level anomaly indicators into engagement-support intelligence within endurance-class ISR pipelines [49]–[52].

XIII. Discussion of Simulation and Experimental Validation Results

The simulation results presented in Section XII and the field validation conducted using the HATSABIBI-26A UAV platform in Section XIII collectively demonstrate the operational feasibility and scalability of the proposed distributed early-warning and cueing architecture for corridor-level ISR support and target-acquisition workflows. Taken together, the results confirm that trigger-driven sensing networks provide measurable improvements in responsiveness, detection continuity, and communication efficiency compared with conventional airborne-only surveillance approaches. This section synthesises the principal findings from both evaluation stages and discusses their implications for distributed ISR pipelines supporting endurance-class loitering munition target acquisition.

A. Consistency Between Simulation Predictions and Flight-Test Observations

A key objective of the experimental campaign described in Section XIII was to verify whether the performance gains predicted in simulation could be reproduced under representative corridor-monitoring conditions. The results demonstrate strong agreement between simulated and measured system behaviour across the primary performance indicators. In particular:

- Decision latency reductions observed experimentally closely matched the **72% improvement** predicted in Section XII,
- Detection persistence increased consistently with node-density scaling assumptions derived from the corridor-coverage continuity condition,
- Cue stability improvements confirmed the effectiveness of neighbourhood consensus validation introduced in Section IV,
- Communication efficiency gains validated the edge-fusion architecture described in Section III.

This correspondence indicates that the simulation framework provides a reliable approximation of distributed trigger-network behaviour across infrastructure-limited monitoring environments.

B. Impact of Trigger-Driven Cueing on ISR Responsiveness

Both simulation and flight-test results confirm that replacing raster-scan airborne surveillance workflows with distributed trigger-driven cue escalation significantly improves anomaly-confirmation responsiveness. Instead of relying on continuous search-pattern coverage, airborne ISR platforms operate as confirmation assets tasked selectively using probabilistically validated anomaly indicators. The latency decomposition model:

$$T_{\text{total}} = T_{\text{detect}} + T_{\text{validate}} + T_{\text{transmit}} + T_{\text{assign}}$$

captures the primary contributors to cue-propagation delay within the proposed architecture. Experimental observations confirmed that reductions in T_{assign} and T_{detect} dominate the overall improvement, because cue-directed waypoint insertion eliminates large-area scanning requirements prior to anomaly verification. These findings support earlier observations that distributed sensing grids enable faster anomaly localisation across extended monitoring corridors than platform-centric surveillance strategies.

C. Detection Persistence as a Function of Sensor-Node Density

Simulation results demonstrated that detection persistence increases monotonically with deployment density:

$$\rho = \frac{N}{A},$$

as predicted by the coverage-continuity condition:

$$d \leq 2R_s.$$

Flight-test observations confirmed that corridor-referenced cueing enabled stable anomaly tracking even when the airborne platform operated outside continuous line-of-sight coverage regions. This behaviour validates the assumption that distributed trigger grids provide persistent observability across terrain-masked environments without requiring continuous overhead ISR presence. The results therefore support the scalability of the architecture for extended corridor-monitoring missions in infrastructure-limited operational theatres.

D. Communication-Efficiency Improvements

Both evaluation stages confirmed that transmitting validated cues rather than raw sensor streams substantially reduces communication bandwidth requirements. The edge-fusion architecture described in Section III enables neighbourhood-level filtering prior to uplink transmission, ensuring that airborne ISR platforms receive only high-confidence anomaly indicators. This reduction in communication load is particularly important for deployments operating in contested electromagnetic environments or regions with limited communications infrastructure. The observed **63% reduction in bandwidth load** therefore represents a critical enabling factor for scalable trigger-grid deployment across geographically dispersed monitoring sectors.

E. GNSS-Degraded Corridor-Tracking Performance

Experimental observations obtained using the HATSABIBI-26A platform confirmed that cue-directed waypoint updates derived from distributed trigger-grid geometry support stable corridor tracking under reduced satellite-navigation availability. These results are consistent with the probabilistic navigation formulation introduced earlier:

$$\hat{x}_k = f(\hat{x}_{k-1}, u_k, z_k),$$

in which cooperative measurement updates compensate for degraded absolute positioning references.
The ability to maintain monitoring continuity under GNSS-degraded conditions represents a critical operational advantage for distributed ISR pipelines operating in contested electromagnetic environments.

F. Validation of Sensor-to-Decision Escalation Workflow

The combined simulation and flight-test results confirm that the hierarchical trigger–fusion–confirmation pipeline supports reliable transformation of terrain-level anomaly detections into engagement-support intelligence. In particular, experimental observations verified the practical applicability of the Bayesian engagement-suitability framework:

$$P(E \mid X) = \frac{P(X \mid E)\,P(E)}{P(X)},$$

introduced in Section X, demonstrating that multi-stage evidence refinement improves classification confidence prior to trajectory retasking decisions. This structured escalation process reduces ambiguity propagation across ISR pipelines and improves overall targeting reliability in distributed surveillance environments.

G. Implications for Endurance-Class ISR Architectures

Taken together, the results presented in Sections XII and XIII demonstrate that distributed trigger-driven surveillance architectures provide a scalable alternative to persistent airborne monitoring for corridor-level anomaly detection and confirmation workflows. The observed reductions in response latency, improvements in detection persistence, and reductions in communication overhead indicate that the proposed architecture can support responsive ISR tasking across extended monitoring sectors while preserving airborne platform endurance for high-confidence confirmation missions. These findings establish the proposed framework as a viable foundation for distributed early-warning and cueing networks supporting next-generation endurance-class ISR and loitering-munition target-acquisition pipelines.

XV. Conclusion

This paper presented a distributed early-warning and cueing architecture integrating RA-IDS-type ground sensor grids with endurance-class loitering munition platforms through probabilistic fusion, neighbourhood consensus validation, adaptive cue prioritisation, and hierarchical ISR–strike decision pipelines. The proposed framework enables transformation of terrain-level anomaly detections into engagement-support intelligence using a structured sensor-to-decision escalation workflow suitable for infrastructure-limited monitoring environments. Analytical modelling demonstrated that distributed trigger-grid deployments satisfying the corridor-coverage continuity condition $d \leq 2R_s$, provide persistent anomaly observability across extended surveillance sectors, while probabilistic cue-ranking and Bayesian engagement-suitability estimation improve classification reliability prior to airborne confirmation assignment. The sensor-to-platform cue-propagation model further showed that trigger-driven escalation architectures significantly reduce response latency compared with conventional airborne-only search workflows.

Simulation-based evaluation confirmed measurable performance improvements across key operational indicators, including a **72% reduction in decision latency**, **31% improvement in detection persistence**, **26% increase in cue stability**, and **63% reduction in communication bandwidth load** relative to raster-scan ISR monitoring baselines. These results were experimentally validated using the HATSABIBI-26A endurance-class UAV platform, which demonstrated reliable cue-directed waypoint retasking performance and stable corridor-tracking capability under distributed trigger-grid guidance conditions, including operation within GNSS-degraded surveillance environments. The integration of multi-

modal sensing vectors, $S_i = \{z_{PIR}, z_{RF}, z_{AC}, z_{MAG}, z_{EO}\}$,
with neighbourhood-level consensus validation and edge-fusion gateways provides a scalable mechanism for maintaining detection continuity across terrain-masked operational corridors without requiring persistent overhead ISR coverage.

This capability supports deployment across mobility-route monitoring scenarios, infrastructure-risk escalation detection environments, and civilian-protection-aligned early-warning architectures requiring low-signature surveillance operation. Collectively, the results establish the proposed distributed trigger-driven architecture as a practical foundation for next-generation corridor-level monitoring systems supporting endurance-class ISR pipelines and probabilistic sensor-to-decision workflows. Future work will extend the framework toward cooperative multi-UAV cue-sharing architectures, adaptive sensor-weight learning using reinforcement-based fusion strategies, and integration with distributed mesh-network command infrastructures supporting resilient operation in contested electromagnetic environments.

REFERENCES

1. Imam, A. S., Surajo, A., Sirajo, B., & Baballe, M. A. (2026). Secure command-and-control data links for long-range loitering munition operations in contested electromagnetic environments. *ICON Journal of Engineering Applications of Artificial Intelligence, 2*(4).
2. Imam, A. S., Surajo, A., & Baballe, M. A. (2026). Distributed probabilistic navigation architectures for endurance-class UAV corridor monitoring. *Global Journal of Research in Engineering: Computer Science and Engineering, 26*(1).
3. Imam, A. S., Sirajo, B., & Surajo, A. (2026). Passive multi-modal target detection architectures for GNSS-denied surveillance environments. *Global Journal of Research in Engineering: Computer Science and Engineering, 26*(2).
4. Imam, A. S., Surajo, A., & Baballe, M. A. (2026). Swarm coordination strategies for distributed ISR corridor monitoring missions. *Global Journal of Research in Engineering: Computer Science and Engineering, 26*(3).
5. Imam, A. S., Surajo, A., & Sirajo, B. (2026). Embedded artificial intelligence perception framework for lightweight surveillance UAV platforms. *Global Journal of Research in Engineering: Computer Science and Engineering, 26*(4).
6. Imam, A. S., Baballe, M. A., & Surajo, A. (2026). Energy-aware trajectory optimisation strategies for endurance-class UAV surveillance missions. *Global Journal of Research in Engineering: Computer Science and Engineering, 26*(5).
7. Hall, D. L., & Llinas, J. (1997). An introduction to multisensor data fusion. *Proceedings of the IEEE, 85*(1), 6–23.
8. Liggins, M. E., II, Hall, D. L., & Llinas, J. (2017). *Handbook of multisensor data fusion*. CRC Press.
9. Bar-Shalom, Y., Li, X. R., & Kirubarajan, T. (2001). *Estimation with applications to tracking and navigation*. Wiley.
10. Blackman, S., & Popoli, R. (1999). *Design and analysis of modern tracking systems*. Artech House.
11. Durrant-Whyte, H., & Bailey, T. (2006). Simultaneous localization and mapping: Part I. *IEEE Robotics & Automation Magazine, 13*(2), 99–110.
12. NATO Science and Technology Organization. (2019). *Distributed intelligence, surveillance and reconnaissance architectures* (STO-TR-IST-160).
13. Elfes, A. (1996). Occupancy grids: A probabilistic framework for robot perception. *Autonomous Robots, 3*, 249–265.
14. Zhao, F., & Guibas, L. (2004). *Wireless sensor networks*. Morgan Kaufmann.
15. Akyildiz, I. F., Su, W., Sankarasubramaniam, Y., & Cayirci, E. (2002). Wireless sensor networks: A survey. *Computer Networks, 38*(4), 393–422.
16. Chong, C. Y., & Kumar, S. P. (2003). Sensor networks: Evolution, opportunities, and challenges. *Proceedings of the IEEE, 91*(8), 1247–1256.
17. Zhang, H., & Hou, J. C. (2005). Maintaining sensing coverage and connectivity in large sensor networks. *Ad Hoc & Sensor Wireless Networks, 7*, 89–124.
18. Mahler, R. (2007). *Statistical multisource-multitarget information fusion*. Artech House.
19. Olfati-Saber, R., Fax, J. A., & Murray, R. M. (2007). Consensus and cooperation in networked multi-agent systems. *Proceedings of the IEEE, 95*(1), 215–233.
20. Cover, T. M., & Thomas, J. A. (2006). *Elements of information theory*. Wiley.
21. Thrun, S., Burgard, W., & Fox, D. (2005). *Probabilistic robotics*. MIT Press.
22. Hero, A. O., & Cochran, D. (2011). Sensor management: Past, present, and future. *IEEE Sensors Journal, 11*(12), 3064–3075.
23. Chen, Y., & Li, Y. (2016). Sensor fusion for target tracking. *IEEE Aerospace and Electronic Systems Magazine, 31*(2), 4–12.
24. Hall, D. L. (2004). *Mathematical techniques in multisensor data fusion*. Artech House.
25. Llinas, J., Bowman, C., & Rogova, G. (1999). Revisiting the JDL data fusion model. *Proceedings of SPIE, 3719*.
26. Pahlavan, K., & Krishnamurthy, P. (2002). *Principles of wireless networks*. Prentice Hall.
27. Gelb, A. (Ed.). (1974). *Applied optimal estimation*. MIT Press.
28. Anderson, B. D. O., & Moore, J. B. (2005). *Optimal filtering*. Dover.
29. Bar-Shalom, Y., & Fortmann, T. E. (1988). *Tracking and data association*. Academic Press.
30. Beard, R. W., & McLain, T. W. (2012). *Small unmanned aircraft: Theory and practice*. Princeton University Press.
31. Chandler, P. R., Rasmussen, S. J., & Pachter, M. (2001). UAV cooperative control. *IEEE Control Systems Magazine,*

21(6), 42–55.
32. Frew, E. W., & Brown, T. X. (2009). Networking issues for small UAVs. *Journal of Intelligent & Robotic Systems, 54*, 21–37.
33. Farrell, J. A. (2008). *Aided navigation: GPS with high-rate sensors*. McGraw-Hill.
34. U.S. Department of Defense. (2018). *Unmanned systems integrated roadmap 2017–2042*.
35. Savkin, A. V., & Huang, H. (2012). Deployment of sensor networks for corridor monitoring. *Robotics and Autonomous Systems, 60*, 1–8.
36. Chong, C. Y., & Kumar, S. (2006). Distributed detection in sensor networks. *IEEE Signal Processing Magazine, 23*(4), 16–25.
37. Wymeersch, H., Lien, J., & Win, M. Z. (2009). Cooperative localization in wireless networks. *Proceedings of the IEEE, 97*(2), 427–450.
38. DARPA. (2019). *Mosaic warfare concept overview*.
39. NATO Science and Technology Organization. (2021). *Sensor-to-shooter integration in distributed ISR* (STO-TR-SAS-123).
40. Russell, S., & Norvig, P. (2021). *Artificial intelligence: A modern approach* (4th ed.).
41. Bishop, C. M. (2006). *Pattern recognition and machine learning*. Springer.
42. Murphy, K. P. (2012). *Machine learning: A probabilistic perspective*. MIT Press.
43. NATO Science and Technology Organization. (2018). *Distributed ISR architectures for coalition operations*.
44. U.S. Army TRADOC. (2018). *Multi-domain operations concept 2035*.
45. Richards, A., & How, J. P. (2002). Aircraft trajectory planning with collision avoidance. *Journal of Guidance, Control, and Dynamics, 25*(4), 755–764.
46. Wang, B. (2011). Coverage problems in sensor networks: A survey. *ACM Computing Surveys, 43*(4).
47. Bai, X., Kumar, S., Xuan, D., Yun, Z., & Lai, T. H. (2010). Coverage and connectivity in sensor deployments. *IEEE Transactions on Mobile Computing, 9*(3), 361–373.
48. Zhang, H., & Hou, J. C. (2006). Is deterministic deployment worse than random deployment? In *Proceedings of IEEE INFOCOM*.
49. Norman, T. L. (2015). Sensor-to-shooter integration architectures. In *IEEE Aerospace Conference*.
50. Clark, J., & Fierro, R. (2007). Cooperative hybrid control of robotic sensor networks. *IEEE Transactions on Robotics, 23*(4), 747–757.
51. NATO Science and Technology Organization. (2021). *ISR integration frameworks for distributed sensing environments*.
52. DARPA. (2020). *Collaborative operations in denied environment (CODE) program overview*.
53. Misra, P., & Enge, P. (2011). *Global positioning system: Signals, measurements and performance*. Ganga-Jamuna Press.
54. Hofmann-Wellenhof, B., Lichtenegger, H., & Collins, J. (2008). *GNSS—Global navigation satellite systems*. Springer.
55. Kaplan, E. D., & Hegarty, C. J. (2017). *Understanding GPS/GNSS: Principles and applications* (3rd ed.). Artech House.
56. Endsley, M. R. (1995). Toward a theory of situation awareness in dynamic systems. *Human Factors, 37*(1), 32–64.
57. Doherty, P., & Rudol, P. (2007). A UAV search and rescue scenario. *AI Magazine, 28*(4), 67–76.
58. NATO Science and Technology Organization. (2022). *Human–machine teaming in autonomous ISR systems* (STO-TR-HFM-245).
59. Krishnamurthy, A. (2005). Adaptive sensor management. *IEEE Signal Processing Magazine, 22*(1), 30–39.
60. Cochran, D. (2007). Sensor resource management. *IEEE Aerospace and Electronic Systems Magazine, 22*(5), 13–18.
61. United Nations Office for the Coordination of Humanitarian Affairs. (2020). *Humanitarian early warning systems framework*.
62. International Committee of the Red Cross. (2021). *Digital technologies and protection in armed conflict*.